
ForeCA: Forecastable Component Analysis

Georg M. Goerg

Carnegie Mellon University, Department of Statistics
 gmg@stat.cmu.edu, www.stat.cmu.edu/~gmg

Abstract

Blind source separation (BSS) techniques are often applied to multivariate time series with the goal to obtain better forecasts. But BSS and the need for better forecasts are often treated separately, in the sense that finding an optimally transformed (sub-)space has nothing to do with the aim to predict well. Here I introduce **Forecastable Component Analysis (ForeCA)**, a new BSS technique for temporally dependent signals that uses forecastability as the explicit objective in finding an optimal transformation. It separates the signal into the forecastable, \mathbf{F} , and the orthogonal white noise space, \mathbf{F}^\perp . Simulations and applications to financial data show that ForeCA successfully finds signals that can be used to forecast. ForeCA therefore automatically discovers informative structure in multivariate signals.

The R package [ForeCA](#) will be publicly available on CRAN upon publication of the manuscript.

1 Introduction

Let $\mathbf{X}(t)$ be n signals observed for $t = 1, \dots, T$. In the general BSS setting,

$$\mathbf{X}(t) = \sum_{j=1}^n \mathbf{a}_j \mathbf{S}_j(t) = \mathbf{A} \mathbf{S}(t), \quad (1)$$

is a mixture of n unobserved sources $\mathbf{S}(t)$, where $\mathbf{A} \in \mathbb{R}^{n \times n}$ is an unknown mixing matrix. BSS aims to estimate a separating matrix $\mathbf{W} \in \mathbb{R}^{n \times n}$ that can recover the sources - up to permutation and scaling -

$$\mathbf{W} \mathbf{X}(t) = \mathbf{W} \mathbf{A} \mathbf{S}(t) = \underbrace{\mathbf{P}}_{\text{permutation}} \underbrace{\mathbf{\Lambda}}_{\text{scaling}} \mathbf{S}(t) \quad (2)$$

Finding the right \mathbf{W} is in this generality ill-posed, because - since we do not know the sources - any invertible \mathbf{A} gives a “solution” $\mathbf{W} = \mathbf{A}^{-1}$. Thus we have to impose some restrictions on \mathbf{A} and $\mathbf{S}(t)$. Typically signals should be “interesting” in some way; there is no point in transforming $\mathbf{X}(t)$ to an arbitrary $\mathbf{S}(t)$ that is less useful, meaningful, interesting, etc. than the original data. Let $\iota(\mathbf{Y})$ measure “interestingness” of the signal \mathbf{Y} . BSS then becomes an optimization problem

$$\widehat{\mathbf{W}} = \arg \max_{\mathbf{W} \in \mathcal{R} \subseteq \mathbb{R}^{n \times n}} \iota(\mathbf{W} \mathbf{X}(t)). \quad (3)$$

Typically restriction is to orthogonal transformations $\mathcal{R} = \{\mathbf{W} \mid \mathbf{W}^\top \mathbf{W} = \mathbf{I}_n\}$. For example, PCA finds large variance sources (Jolliffe, 2002) - $\iota(X) = \mathbb{E}(X - \mu)^2$ in (3)-; independent component analysis (ICA) finds statistically independent sources (Hyvärinen and Oja, 2000); the recently introduced slow feature analysis (SFA) (Wiskott and Sejnowski, 2002) tries to find “slow” signals and is equivalent to maximizing the lag 1 correlation coefficient.

Often sources are estimated and then predictions are made through them - hoping that forecasting on the lower-dimensional feature space $\mathbf{S}(t)$ is more accurate, simpler, more efficient, etc. than on the original $\mathbf{X}(t)$ space. However, standard BSS techniques such as PCA, SFA, or ICA do not explicitly address forecastability of the sources. For example, just because a signal has high variance does not mean it is easy to forecast.

Thus let's define interesting as having predictive power. Forecasting a sequence by its history is not only good for its own sake (finance, economics), but even when future values are not immediately interesting, signals that do have predictive power exhibit non-trivial structure by definition - and are therefore easier to interpret. For example, the real world time series¹ in Fig. 1 are ordered from least (S&P500 daily returns) to most forecastable (monthly temperature in Nottingham) according to the ForeCA forecastability measure $\Omega(x_t)$ (introduced in Definition 3.1 below). And indeed moving from left to right the series exhibit more structure.

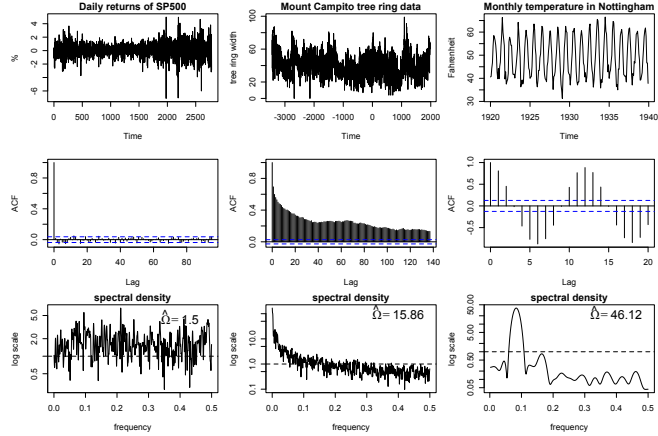


Figure 1: (left to right) i) S&P 500 daily returns; ii) Mount Campito tree ring series; iii) monthly mean temperatures in Nottingham. (top) observed time series; (middle) sample ACF $\hat{\rho}(k)$; (bottom) smoothed spectral density estimate $\tilde{I}_x(\omega_j)$ and $\hat{\Omega}(x_t)$ (in %).

The main contributions of this paper are i) a measure of forecastability for (stationary) time series, ii) a new BSS technique, ForeCA, that can recover forecastable signals, iii) an iterative algorithm that provably converges to local optima, and iv) simulations and applications showing that ForeCA outperforms PCA, SFA, and ICA in finding low-dimensional, but still forecastable sub-spaces.

2 Time series preliminaries

Let y_t be a univariate, second-order stationary time series with mean $\mathbb{E}y_t = \mu_y < \infty$, variance $\mathbb{V}y_t = \sigma_y^2 < \infty$, and autocovariance function (ACVF)

$$\gamma_y(k) = \mathbb{E}(y_t - \mu_y)(y_{t-k} - \mu_y). \quad (4)$$

The ACVF for univariate processes is symmetric in k , $\gamma_y(k) = \gamma_y(-k)$. Let $\rho(k) = \gamma(k)/\gamma(0)$ be the autocorrelation function (ACF). A large $\rho(k)$ means that the process k time steps ago has a large influence on the present t . The sample ACFs $\hat{\rho}(k)$ in Fig. 1 show that e.g. S&P 500 daily returns are uncorrelated with their own past (stock market efficiency); yearly tree ring growth is highly correlated over time with significant lags even for $k \geq 100$ years; and intuitively temperature in month t is highly correlated with the temperature $k = 6$ (cold \leftrightarrow warm) and $k = 12$ (cold \rightarrow cold; warm \rightarrow warm) months ago (or in the future).

The building block of time series models is *white noise* ε_t , which has zero mean, finite variance, and is uncorrelated over time: $\varepsilon_t \sim WN(0, \sigma_\varepsilon^2)$ iff i) $\mathbb{E}\varepsilon_t = 0$, ii) $\mathbb{V}\varepsilon_t = \gamma_\varepsilon(0) = \sigma_\varepsilon^2$, and iii) $\gamma_\varepsilon(k) = 0$ if $k \neq 0$. Only if ε_t is a Gaussian process, then it is also independent over time. For example, the S&P 500 returns are uncorrelated, but their variance is clearly clustering in time and thus not uncorrelated. Hence they are not independent and thus not Gaussian (also, kurtosis ≈ 7.71).

For multivariate second-order stationary $\{\mathbf{X}_t \mid t \in \mathbb{Z}\}$ with mean $\mathbb{E}\mathbf{X}_t = \boldsymbol{\mu} \in \mathbb{R}^n$,² the ACVF

$$\mathbb{R}^{n \times n} \ni \boldsymbol{\Gamma}_X(k) = \mathbb{E}(\mathbf{X}_t - \boldsymbol{\mu})(\mathbf{X}_{t-k} - \boldsymbol{\mu})^\top, \quad k \in \mathbb{Z}, \quad (5)$$

is a matrix-valued function of k . In particular, $\boldsymbol{\Gamma}_X(0) = \boldsymbol{\Sigma}_X$ is the covariance matrix. The diagonal of $\boldsymbol{\Gamma}_X(k)$ contains the ACVF of each $\mathbf{X}_i(t)$, $i = 1, \dots, n$; the off-diagonal element (i, j)

$$\gamma_{ij}(k) = \boldsymbol{\Gamma}_X(k)_{(i,j)} = \mathbb{E}(\mathbf{X}_{i,t} - \boldsymbol{\mu}_i)(\mathbf{X}_{j,t-k} - \boldsymbol{\mu}_j) \in \mathbb{R}, \quad (6)$$

¹For data sources see Appendix A.

²Without loss of generality (WLOG) assume $\boldsymbol{\mu} = \mathbf{0}$.

is the cross-covariance between the i th and j th series at lag k . Contrary to $\gamma_y(k)$, $\mathbf{\Gamma}_X(k)$ is not symmetric but

$$\mathbf{\Gamma}_X(k) = \mathbf{\Gamma}_X(-k)^\top. \quad (7)$$

2.1 Spectrum and spectral density

The spectrum³ of a stationary process can be defined as the Fourier transform⁴ of its ACVF,

$$S_y(\lambda) = \frac{1}{2\pi} \sum_{j=-\infty}^{\infty} \gamma_y(j) e^{2\pi i j \lambda}, \quad \lambda \in [-\pi, \pi], \quad (8)$$

where $i = \sqrt{-1}$ is the imaginary unit. Since $\gamma_y(k)$ is symmetric, the spectrum is a real-valued, non-negative function, $S_y : [-\pi, \pi] \rightarrow \mathbb{R}^+$. The spectrum contains the same information as the ACVF, but in a different way. For white noise ε_t all $\gamma_\varepsilon(k) = 0$ if $k \neq 0$, thus its spectrum is simply a constant, $S_\varepsilon(\lambda) = \frac{\sigma_\varepsilon^2}{2\pi}$ for all $\lambda \in [-\pi, \pi]$. When $\gamma(k) > 0$ for $k \neq 0$ - which can be modeled and then used for prediction - the spectrum has peaks at the corresponding frequencies. For example, the spectral density of monthly temperature series (right in Fig. 1) has large peaks at $\lambda \approx 1/6$ and $1/12$, which corresponds to the 1 year and half-year cycle.

Vice versa, the ACVF can be recovered from the spectrum using the inverse Fourier transform

$$\gamma_y(k) = \int_{-\pi}^{\pi} S_y(\lambda) e^{-i2\pi k \lambda} d\lambda, \quad k \in \mathbb{Z}. \quad (9)$$

In particular, $\int_{-\pi}^{\pi} S_y(\lambda) d\lambda = \sigma_y^2$. Let

$$f_y(\lambda) = \frac{S_y(\lambda)}{\sigma_y^2} = \frac{1}{2\pi} \sum_{j=-\infty}^{\infty} \rho_y(j) e^{2\pi i j \lambda}, \quad \lambda \in [-\pi, \pi], \quad (10)$$

be the *spectral density* of y_t . As $f_y(\lambda) \geq 0$ and $\int_{-\pi}^{\pi} f_y(\lambda) d\lambda = 1$, the spectral density can be interpreted as a probability density function (pdf) of an (unobserved) random variable (RV) Λ that ‘‘lives’’ on the unit circle (parametrized by $\lambda \in [-\pi, \pi]$). For white noise $f_\varepsilon(\lambda) = \frac{1}{2\pi}$ is the uniform distribution $U(-\pi, \pi)$.

2.2 Spectrum of multivariate processes and linear combinations

For multivariate $\mathbf{X}_t \in \mathbb{R}^n$ the spectrum equals

$$S_X(\lambda) = \frac{1}{2\pi} \sum_{k=-\infty}^{\infty} \mathbf{\Gamma}_X(k) e^{2\pi i k \lambda}, \quad \lambda \in [-\pi, \pi]. \quad (11)$$

Contrary to the univariate case, (11) is in general complex-valued (in the off-diagonals). However, since $\mathbf{\Gamma}_X(k) = \mathbf{\Gamma}_X(-k)^\top$ also $S_X(\lambda) \in \mathbb{C}^{n \times n}$ is Hermitian for every $\lambda \in [-\pi, \pi]$ (Brockwell and Davis, 1991, p. 436)

$$S_X(\lambda) = S_X(\lambda)^H = \overline{S_X(\lambda)^\top}, \quad (12)$$

where $\bar{z} = a - ib$ is the complex conjugate $z = a + ib \in \mathbb{C}$. Therefore $S_X(\lambda)$ is semi-positive definite; in particular $\mathbf{w}^\top S_X(\lambda) \mathbf{w} \geq 0$ for all $\mathbf{w} \in \mathbb{R}^n$.

For dimension reduction we consider linear combinations $y_t = \mathbf{w}^\top \mathbf{X}_t$, $\mathbf{w} \in \mathbb{R}^n$. By assumption $\mathbb{E}y_t = \mathbf{w}^\top \mathbb{E}\mathbf{X}_t = 0$ and $\gamma_y(k) = \mathbb{E}y_t y_{t-k} = \mathbf{w}^\top \mathbf{\Gamma}_X(k) \mathbf{w}$. In particular, $\gamma_y(0) = \sigma_y^2 = \mathbf{w}^\top \Sigma_X \mathbf{w}$. The spectrum of $\mathbf{w}^\top \mathbf{X}_t$ can be quickly computed via $S_y(\lambda) = \mathbf{w}^\top S_X(\lambda) \mathbf{w}$ and consequently

$$f_y(\lambda) = \frac{\mathbf{w}^\top S_X(\lambda) \mathbf{w}}{\mathbf{w}^\top \Sigma_X \mathbf{w}}. \quad (13)$$

³In the time series literature (8) is often called the spectral density. In this work I reserve the term *spectral density* for the normalized spectrum $f_y(\lambda) := S_y(\lambda)/\sigma_y^2$ in (10), as it integrates to one such as standard probability density functions.

⁴It converges point-wise if $\sum_{k=-\infty}^{\infty} \|\mathbf{\Gamma}_X(k)\|_F < \infty$; it converges in least-squares sense if $\sum_{k=-\infty}^{\infty} \|\mathbf{\Gamma}_X(k)\|_F^2 < \infty$. Standard stationary process such as auto-regressive processes of order p ($AR(p)$) satisfy the point-wise criterion; long memory processes such as fractional noise satisfy the second.

3 Measuring forecastability of stationary processes

Forecasting is inherently embedded in the time domain. Yet, since the spectrum \leftrightarrow ACVF provides a one-to-one way to go back and forth between the time and frequency domain, we can use frequency domain properties to measure forecastability.

The intuition for the here proposed measure of forecastability is as follows. Consider $y_t = \sqrt{2} \cos(2\pi\mathcal{Y}t + \theta)$, where $\theta \sim U(-\pi, \pi)$. Imagine someone picks \mathcal{Y} at random according to $p_{\mathcal{Y}}(y)$ independent of θ . If we have to make a prediction about the future before seeing the data (and before seeing the picked \mathcal{Y}), then uncertainty about the future of y_t is manifested in the uncertainty about \mathcal{Y} (since $\cos(2\pi\mathcal{Y}t + \theta)$ is a deterministic function of t). One can show that $S_y(\lambda) = p_{\mathcal{Y}}(\lambda)$ (Gibson, 1994). For finite support distribution the maximum entropy occurs for the uniform distribution; thus a flat spectrum should indicate the least predictable sequence. And indeed, a flat spectrum corresponds to white noise which by definition is unpredictable (using linear predictors). The less uncertain we are about \mathcal{Y} the less uncertain we are about future y_{t+h} .

It is therefore natural to measure uncertainty about the future as the *spectral entropy* of $f_y(\lambda)$,

$$H_{s,a}(y_t) := - \int_{-\pi}^{\pi} f_y(\lambda) \log_a f_y(\lambda) d\lambda. \quad (14)$$

where a is an arbitrary logarithm base (typically, $a = 2$ or $a = e$). Since entropy over a bounded interval $[a, b]$ achieves its maximum for the uniform distribution, $U(a, b)$, for any stationary process y_t

$$H_{s,a}(y_t) \leq H_{s,a}(\text{white noise}) = - \int_{-\pi}^{\pi} \frac{1}{2\pi} \log_a \frac{1}{2\pi} d\lambda = \log_a 2\pi. \quad (15)$$

with equality if only if y_t is white noise.

Definition 3.1 (Forecastability of a stationary process). *For a second-order stationary process y_t , let*

$$\Omega : y_t \mapsto [0, 1], \quad \Omega(y_t) := 1 - \frac{H_{s,a}(y_t)}{\log_a(2\pi)} = 1 - H_{s,2\pi}(y_t), \quad (16)$$

be the forecastability of y_t .

This ForeCA measure $\Omega(y_t)$ relies on Gaussianity as only then $f_y(\lambda)$ fully captures the temporal properties of y_t . While time series are often non-Gaussian, ForeCA can be seen as a computationally and algebraically manageable forecastability measure - in a similar way as PCA is extensively used for iid data, even though not necessarily Gaussian.

Properties 3.2 (Properties of Ω).

1. $\Omega(\text{iid}) = 0$ and $\Omega(x_t) = 1$ if x_t is a (countable) sum of sinusoids.
2. *invariant to scaling and shifting*: $\Omega(ay_t + b) = \Omega(y_t)$ for $a, b \in \mathbb{R}$, $a \neq 0$.
3. *max subadditivity for uncorrelated processes*:

$$\Omega(\alpha x_t + \sqrt{1 - \alpha^2} y_t) \leq \max\{\Omega(x_t), \Omega(y_t)\} \text{ if } \mathbb{E}x_t y_s = 0 \text{ for all } s, t \in \mathbb{Z}. \quad (17)$$

Property 3 seems to let a maximization problem only have a trivial boundary solution. However, Eq. (17) only holds if the processes are uncorrelated. But it is intuitively clear that combining uncorrelated series does not make prediction easier; in general it will be harder to forecast (think of e.g. signal + noise). However, if $\mathbb{E}x_t y_s \neq 0$ for some $s, t \in \mathbb{Z}$ then combining two series can make prediction easier: $\Omega(\alpha x_t + \sqrt{1 - \alpha^2} y_t) > \max\{\Omega(x_t), \Omega(y_t)\}$ is possible for some $\alpha \in (0, 1)$.

The three time series in Fig. 1 are ordered (left to right) by increasing forecastability and indeed larger $\widehat{\Omega}$ correspond to intuitively more predictable real-world phenomena (stock returns are in general not predictable; monthly temperature is). We can thus use (16) to guide the search for optimal \mathbf{w} that make $y_t = \mathbf{w}^\top \mathbf{X}_t$ as forecastable as possible.

3.1 Plug-in estimator for Ω

To estimate $\Omega(x_t)$ first estimate the spectrum $S_x(\lambda)$, normalize it, and then plug it in (14). An unbiased estimator of $S_x(\lambda)$ is the periodogram (or power spectrum)

$$I_{T,x}(\omega_j) := |X(\omega_j)|^2 = \left| \frac{1}{\sqrt{T}} \sum_{k=0}^{T-1} x_k e^{-2\pi i \omega_j k} \right|^2, \quad \omega_j = j/T, \quad j = 0, 1, \dots, T-1 \quad (18)$$

where ω_j are the Fourier frequencies (scaled by 2π for easier interpretation). Normalized periodograms $\tilde{I}_{j,x} = \frac{I_{T,x}(\omega_j)}{\sum_{j=0}^{T-1} I_{T,x}(\omega_j)}$ are shown in Figure 1 (bottom). Plug-in estimates obtained via

$$\hat{\Omega}(x_t) = 1 - \sum_{j=1}^{T-1} \tilde{I}_{j,x} \cdot \log_{a=T} \left(\tilde{I}_{j,x} \right) \quad (19)$$

are shown in the top right corner (in %). Note that usually an entropy estimator would average solely over $\log f(x_j)$ without multiplicative $f(x_j)$ terms. This however assumes that the data points x_j are sampled from $f(x)$ (and thus the central limit theorem would give $\frac{1}{n} \sum_{i=1}^n \log f(x_i) \rightarrow \mathbb{E}_f \log f(x) = \int f(x) \log f(x) dx$). While this is true in the traditional statistical framework, here the “data points” are the Fourier frequencies ω_j and the fast Fourier transform (FFT) samples them uniformly (and deterministically) from $[-\pi, \pi]$ and not according to the “true” spectral density.⁵

The estimator in (19) can be improved by a better spectral density estimation (Fryzlewicz, Piotr, Nason, Guy, Vonsachs, and Rainer, 2008; Lees and Park, 1995; Trobs and Heinzl, 2006) and better entropy estimates (Paninski, 2003). Future research can also focus on direct spectral entropy estimation without estimating densities first - as is common for traditional entropy estimation (Sricharan, Raich, and Hero, 2011; Stowell and Plumbley, 2009). However, since neither power spectrum nor entropy estimation are the primary focus of this work, we will use standard⁶ estimators for $S_y(\lambda)$ and then the plug-in estimator of (19) - which for a discrete RV is at least universally consistent (Antos and Kontoyiannis, 2001). Simulations as well as applications show that it gives reasonable estimates and we do not expect the results to change qualitatively for other estimators.

4 Maximizing forecastability

The BSS optimization problem for ForeCA becomes

$$\max_{\mathbf{w}} \Omega(\mathbf{w}^\top \mathbf{X}_t) = \max_{\mathbf{w}} \left(1 - \frac{\int_{-\pi}^{\pi} f_y(\lambda) \log_a f_y(\lambda) d\lambda}{\log_a(2\pi)} \right), \quad (20)$$

$$\text{subject to } \mathbf{w}^\top \Sigma_X \mathbf{w} = 1, \quad (21)$$

where (21) must hold since (14) uses the spectral density of y_t , i.e. we need $\mathbb{V}y_t = \mathbf{w}^\top \Sigma_X \mathbf{w} = 1$.

Since forecastability is invariant to shift and scale, we shall not only assume zero mean, but also that the observed signals are contemporaneously uncorrelated and have unit variance in each component. WLOG consider $\mathbf{U}(t) = \Sigma_X^{-1/2} \mathbf{X}(t)$; thus $\mathbb{E}\mathbf{U}\mathbf{U}^\top = \mathbf{I}_n$. Given the optimal unmixing matrix $\widehat{\mathbf{W}}_U$ for $\mathbf{U}(t)$, the original separating matrix becomes $\widehat{\mathbf{W}}_X = \widehat{\mathbf{W}}_U \widehat{\Sigma}_X^{-1/2}$. The solution to (20) is then equivalent to

$$\mathbf{w}^* = \arg \max_{\mathbf{w}} \int_{-\pi}^{\pi} (\mathbf{w}^\top S_U(\lambda) \mathbf{w}) (\log [\mathbf{w}^\top S_U(\lambda) \mathbf{w}]) d\lambda, \quad \text{s.t. } \mathbf{w}^\top \mathbf{w} = 1. \quad (22)$$

Using the periodogram $\widehat{S}_U(\omega_j) \in \mathbb{C}^{n \times n}$, $j = 0, \dots, T-1$, (22) becomes a sum and thus

$$\mathbf{w}^* = \arg \max_{\mathbf{w}} \sum_{j=0}^{T-1} \left(\mathbf{w}^\top \widehat{S}_U(\omega_j) \mathbf{w} \right) \left(\log [\mathbf{w}^\top \widehat{S}_U(\omega_j) \mathbf{w}] \right), \quad \text{s.t. } \mathbf{w}^\top \mathbf{w} = 1. \quad (23)$$

⁵Recent advances in “compressed sensing” (see Jacques and Vandergheynst, 2010, for a survey) can probably improved estimates; see also “non-uniform Fourier transforms” (Fessler and Sutton, 2003).

⁶For the simulations and applications we use smoothed estimators from the R (R Development Core Team, 2010) package `sapa: SDF(y, method = 'multitaper')`.

Here $\widehat{S}_U(\omega_j) \in \mathbb{C}^{n \times n}$ varies with ω_j while $\mathbf{w} \in \mathbb{R}^n$ is globally constant - which makes it difficult to obtain an analytic, closed-form solution. However, (23) can be solved iteratively borrowing ideas from the Expectation Maximization (EM) algorithm (Dempster, Laird, and Rubin, 1977).

4.1 Solving the optimization problem via an EM-type algorithm

Let $h(\mathbf{w}) = \sum_{j=1}^{T-1} \mathbf{w}^\top \widehat{S}_U(\omega_j) \mathbf{w} \cdot \log [\mathbf{w}^\top \widehat{S}_U(\omega_j) \mathbf{w}]$. For every $\mathbf{w} \in \mathbb{R}^n$, $\|\mathbf{w}\|_2 = 1$, $h(\mathbf{w})$ has the form of a mixture model with weights $\pi(j | \mathbf{w}) := \mathbf{w}^\top \widehat{S}_U(\omega_j) \mathbf{w} \geq 0$ and “log-likelihood” $\ell(\mathbf{w}; \omega_j) := \log [\mathbf{w}^\top \widehat{S}_U(\omega_j) \mathbf{w}] = \log f_{\mathbf{w}^\top \mathbf{X}_t}(\omega_j)$. Just as in an EM algorithm $h(\mathbf{w})$ can be maximized iteratively by

$$\mathbf{w}_{i+1} = \arg \max_{\mathbf{w}} \mathbf{w}^\top \overline{\widehat{S}_U^{(i)}} \mathbf{w}, \quad (24)$$

where $\overline{\widehat{S}_U^{(i)}} = \sum_{j=0}^{T-1} \widehat{S}_U^{(i)}(\omega_j)$ and $\widehat{S}_U^{(i)}(\omega_j) = \widehat{S}_U(\omega_j) \cdot \ell(\mathbf{w}_i; \omega_j)$. Eq. (24) can be solved analytically by the first eigenvector of $\overline{\widehat{S}_U^{(i)}}$ - which automatically guarantees $\|\mathbf{w}\|_2 = 1$. The procedure iterates until $\|\mathbf{w}_{i+1} - \mathbf{w}_i\| < tol$ for some tolerance level tol . To initialize sample \mathbf{w}_0 from an n -dimensional uniform hyper-cube, $U_n(-1, 1)$, and normalize to $\mathbf{w}_0 = \mathbf{w}_0 / \sqrt{\sum_{j=1}^n w_{j,0}^2}$.

Theorem 4.1 (Convergence). *The sequence of \mathbf{w}_i , $i = 0, 1, 2, \dots$ obtained via (24) converges to a local maximum $h(\mathbf{w}^*)$, where $\lim_{i \rightarrow \infty} \mathbf{w}_i = \mathbf{w}^*$.*

Proof. The entropy of a discrete RVs taking values in a finite alphabet $\{\omega_0, \dots, \omega_{T-1}\}$ is bounded below by zero and above by $\log_a T$; thus $-\log_a T \leq h(\mathbf{w}) \leq 0$ for all $\mathbf{w} \in \mathbb{R}^n$. For convergence it remains to be shown that $h(\mathbf{w}_{i+1}) \geq h(\mathbf{w}_i)$ with equality if and only if $\mathbf{w}_{i+1} = \mathbf{w}_i = \mathbf{w}^*$.

$$h(\mathbf{w}_i) = \sum_{j=1}^{T-1} \mathbf{w}_i^\top S_U(\omega_j) \mathbf{w}_i \cdot \ell(\mathbf{w}_i; \omega_j) = \mathbf{w}_i^\top \overline{\widehat{S}_U^{(i)}} \mathbf{w}_i \quad (25)$$

$$\leq \mathbf{w}_{i+1}^\top \overline{\widehat{S}_U^{(i)}} \mathbf{w}_{i+1} = \sum_{j=1}^{T-1} \mathbf{w}_{i+1}^\top S_U(\omega_j) \mathbf{w}_{i+1} \cdot \log [\mathbf{w}_i^\top S_U(\omega_j) \mathbf{w}_i] \quad (26)$$

$$\leq \sum_{j=1}^{T-1} \mathbf{w}_{i+1}^\top S_U(\omega_j) \mathbf{w}_{i+1} \cdot \log [\mathbf{w}_{i+1}^\top S_U(\omega_j) \mathbf{w}_{i+1}] = h(\mathbf{w}_{i+1}) \quad (27)$$

where (26) follows as \mathbf{w}_{i+1} is the first eigenvector of $\overline{\widehat{S}_U^{(i)}}$, and (27) holds as $\mathbb{E}_p \log q = \sum_{j=1}^n p_j \log q_j \leq \sum_{j=1}^n p_j \log p_j = \mathbb{E}_p \log p$ for any $q \neq p$. \square

To prevent bad local optima one can repeat (24) for several random starting positions \mathbf{w}_0 and then use the best solution over all local optima.

5 Simulations

Here we analyze the linear mixture (each row has unit norm)

$$\mathbf{A} = \begin{pmatrix} 0.22 & 0.87 & 0.44 \\ 0.41 & -0.82 & 0.41 \\ -0.27 & 0.53 & 0.80 \end{pmatrix}, \quad (28)$$

of three sources $\mathbf{S} \in \mathbb{R}^{3 \times 1000}$: i) $AR(1)$ $x_t = \phi_1 x_{t-1} + \varepsilon_t$ with $\phi_1 = 0.9$, ii) white noise, and iii) an $MA(2)$ $x_t = \varepsilon_t + \theta_2 \varepsilon_{t-2}$ with $\theta_2 = -0.5$. Figure 2 shows the simulated sources, the mixture $\mathbf{X} = \mathbf{A}\mathbf{S}$, and their sample ACFs. The diagonal ACFs in Fig. 2b have characteristic $AR(1)$, white noise, and $MA(2)$ sample moments; all lags in the off-diagonal are non-significant since sources were generated independently. The mixtures, however, do not have this clearly separated structure anymore: the diagonal does not show a lot of correlation per signal, and the off-diagonal lags are

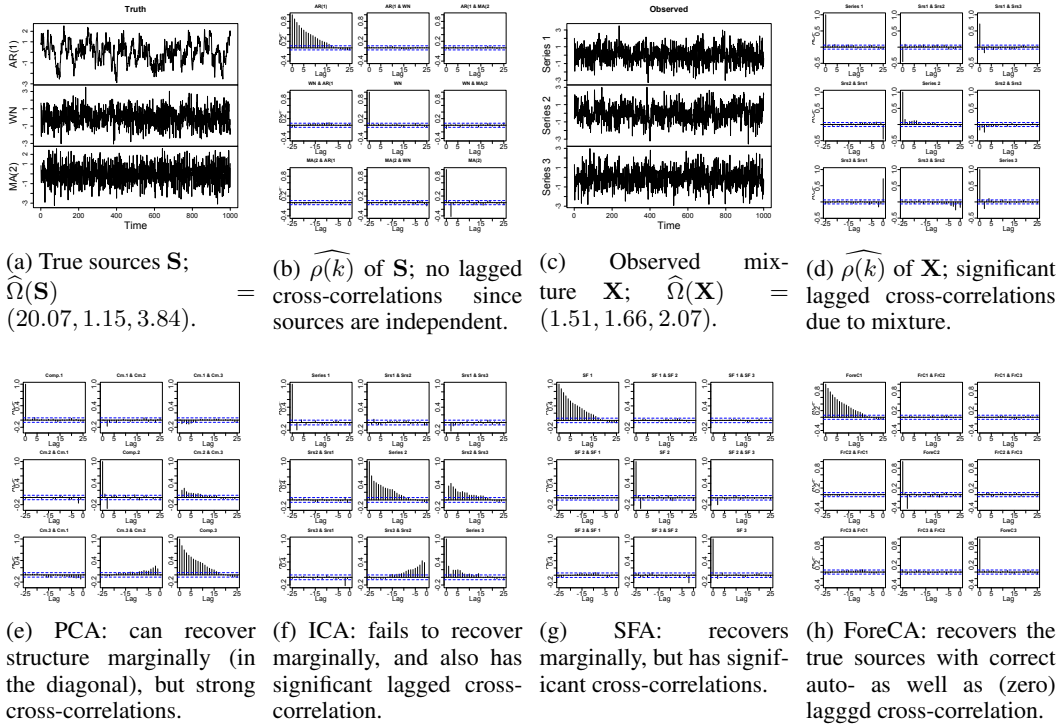


Figure 2: (top left) Independent, but autocorrelated sources \mathbf{S} ; (top right) mixtures $\mathbf{X} = \mathbf{A}\mathbf{S}$ and their autocorrelations, and (bottom) sample ACF of sources \mathbf{X} from PCA, ICA, SFA, and ForeCA.

now significant. Thus while the sources could be forecasted independently using simple models, the observed mixture would have to be modeled with a VAR and many more parameters.

A better (lower-dimensional) representation of \mathbf{X} should at least - if not recovering the true \mathbf{S} - decrease the number of parameters to model multivariate autocorrelations. The bottom row of Fig. 2 shows the sample ACF of the recovered components via PCA, ICA, SFA, and ForeCA. Since PCA, SFA, and ICA ignore temporal dependencies, they fail to separate the signals in not cross-correlated sources. While PCA and SFA can at least marginally recover the sources correctly (diagonal ACF have white noise, $AR(1)$ and $MA(2)$ properties), ICA even fails to achieve that. Fitting a VAR to the ICs would yield more complex models than VAR fits to the original data \mathbf{X} . ForeCA can recover the true sources and thus provides a good starting point for parsimonious VAR models (or even independent AR models on each single time series). Note that PCA yields white noise as the most important signal; however as pointed out above, just because a signal has large variance does not mean it is easy to forecast.

6 Applications

Figure 3a shows daily returns of eight equity funds from 2002/01/01 to 2007/05/31 ($T = 1413$ observations). In the financial context finding forecastable series is a reasonable goal by itself, not just for structure discovery. In particular, we can interpret a linear combination \mathbf{w} as a portfolio of stocks. The \mathbf{w}^* with the highest Ω gives the most forecastable portfolio.

Figure 3b shows a bi-plot for PCA and ForeCA for $(\mathbf{w}_1, \mathbf{w}_2)$ and $(\mathbf{w}_3, \mathbf{w}_4)$. As PC 1 assign approximately equal weight to all funds, it represents the average market movement; the second component contrasts Gold & Mining versus the rest and we can therefore label it as the commodity source. The third and fourth component represent geographic regions.

However, even though the high-variance market movement (PC 1) is also the most predictable PC, it is just slightly more predictable than the most forecastable fund, India (scree-plot in Fig. 3c).

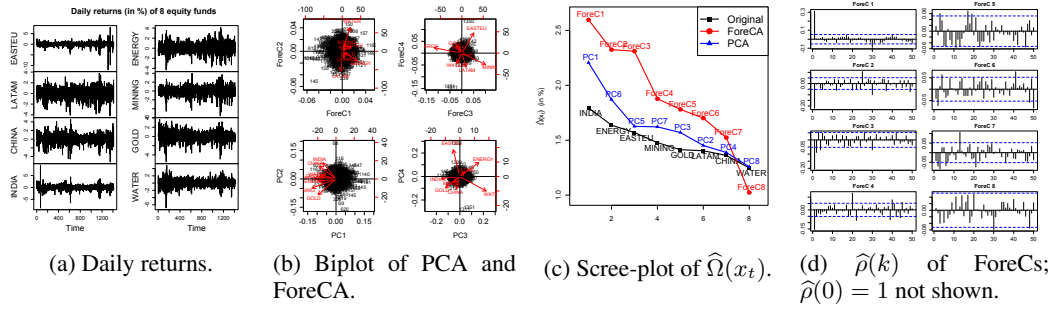


Figure 3: Equity fund returns analyzed with PCA and ForeCA.

On the other hand, a portfolio that combines Water (weight $w_{water,1} = 0.31$) with Eastern Europe (0.32), India (0.23) & Energy (0.40) is about twice as forecastable as India (these weights are those of ForeC 1 - see the bi-plot in Fig. 3b). The second ForeC also achieves substantial forecastability by selling the LATAM (-0.73) and buying Water (0.91) fund (or vice versa). Lastly, the third ForeC combines Energy and Mining - clearly two dependent areas that can be hedged against each other.

7 Related work

In the classic time series literature [Box and Tiao \(1977\)](#) introduced canonical analysis and measure predictive power by the residual variance of fitting vector auto-regression (VAR) models to the data. Recently [Matteson and Tsay \(2011\)](#) propose another time series BSS technique that blends PCA and ICA, as it separates signals to the extent of 4th moments (but not higher).

Remark 7.1. *The entropy rate of a Gaussian process with ACVF $\gamma_y(k)$ is related to the spectrum via ([Cover and Thomas, 1991](#), p. 417)*

$$\mathcal{H}(y_t) = \lim_{t \rightarrow \infty} H(y_t | y_{t-1}, y_{t-2}, \dots) = \frac{1}{2} \log 2\pi e + \frac{1}{4\pi} \int_{-\pi}^{\pi} \log S_y(\lambda) d\lambda. \quad (29)$$

[Gomez-Herrero, Rutanen, and Egiazarian \(2010\)](#); [Li and Adali \(2010\)](#) take a similar BSS approach by minimizing the entropy rate of the sources, but they also require VAR model fitting and/or numerical optimization. On the contrary, ForeCA is non-parametric and has a fast analytic (iterative) solution. Moreover, even though $\Omega(x_t)$ resembles (29) closely, it is based on the (classic) iid entropy of the spectral density, which we believe has a more accessible interpretation ([Gibson, 1994](#); [Gibson, Stanners, and McClellan, 1993](#)). It can also benefit from the extensive literature on frequency domain properties of time series.

8 Discussion

I introduce forecastable component analysis (ForeCA) - a new BSS technique for temporally dependent signals. Contrary to other BSS methods - such as PCA or ICA - ForeCA actively takes temporal dependence into account and searches for the most forecastable sub-space. It does this by estimating the entropy of the frequency spectrum; the lower the entropy the more forecastable is the signal. The optimization problem has an iterative, yet fast analytic solution, and provably leads to a (local) optimum. Simulations and applications to financial data confirm that ForeCA is better than PCA, SFA, or ICA at finding the most predictable signals.

A Data sources

All datasets are publicly available from R packages ([R Development Core Team, 2010](#)).

Figure 1: SP500 in MASS; camp in tseries; nottem in datasets.

Figure 3: equityFunds in fEcofin.

References

- Antos, A. and I. Kontoyiannis (2001). Estimating the entropy of discrete distributions. In *Information Theory, 2001. Proceedings. 2001 IEEE International Symposium on*, pp. 45.
- Box, G. E. P. and G. C. Tiao (1977). A canonical analysis of multiple time series. *Biometrika* 64(2), 355–365.
- Brockwell, P. J. and R. A. Davis (1991). *Time series: Theory and methods* (2nd ed.). Springer Series in Statistics.
- Cover, T. M. and J. Thomas (1991). *Elements of Information Theory*. Wiley.
- Dempster, A. P., N. M. Laird, and D. B. Rubin (1977). Maximum likelihood from incomplete data via the EM algorithm. *Journal of the Royal Statistical Society Series B Methodological* 39(1), 1–38.
- Fessler, J. A. and B. P. Sutton (2003). Nonuniform fast fourier transforms using min-max interpolation. *IEEE Trans. Signal Process* 51, 560–574.
- Fryzlewicz, Piotr, Nason, P. Guy, Vonsachs, and Rainer (2008, September). A wavelet-Fisz approach to spectrum estimation. *Journal of Time Series Analysis* 29(5), 868–880.
- Gibson, J. (1994). What is the interpretation of spectral entropy? In *Information Theory, 1994. Proceedings., 1994 IEEE International Symposium on*, pp. 440.
- Gibson, J., S. Stanners, and S. McClellan (1993). Spectral entropy and coefficient rate for speech coding. In *Signals, Systems and Computers, 1993. 1993 Conference Record of The Twenty-Seventh Asilomar Conference on*, pp. 925–929 vol.2.
- Gomez-Herrero, G., K. Rutanen, and K. Egiazarian (2010). Blind source separation by entropy rate minimization. *Signal Processing Letters, IEEE* 17(2), 153–156.
- Hyvärinen, A. and E. Oja (2000). Independent component analysis: algorithms and applications. *Neural Networks* 13, 411–430.
- Jacques, L. and P. Vandergheynst (2010). Compressed Sensing : “When sparsity meets sampling”. *Signal Processing*, 1–30.
- Jolliffe, I. T. (2002). *Principal Component Analysis* (Second ed.). Springer.
- Lees, J. M. and J. Park (1995). Multiple-taper spectral-analysis - a stand-alone c-subroutine. *Computers Geosciences* 21(2), 199–236.
- Li, X.-L. and T. Adali (2010). Blind spatiotemporal separation of second and/or higher-order correlated sources by entropy rate minimization. In *Acoustics Speech and Signal Processing (ICASSP), 2010 IEEE International Conference on*, pp. 1934–1937.
- Matteson, D. S. and R. S. Tsay (2011). Dynamic orthogonal components for multivariate time series. *Journal of the American Statistical Association* 106(496), 1450–1463.
- Paninski, L. (2003, June). Estimation of entropy and mutual information. *Neural Comput.* 15(6), 1191–1253.
- R Development Core Team (2010). *R: A Language and Environment for Statistical Computing*. Vienna, Austria: R Foundation for Statistical Computing. ISBN 3-900051-07-0.
- Sricharan, K., R. Raich, and A. Hero (2011). K-nearest neighbor estimation of entropies with confidence. In *Information Theory Proceedings (ISIT), 2011 IEEE International Symposium on*, pp. 1205–1209.
- Stowell, D. and M. D. Plumbley (2009). Fast Multidimensional Entropy Estimation by k-d Partitioning. *IEEE Signal Processing Letters* 16, 537–540.
- Trobs, M. and G. Heinzel (2006). Improved spectrum estimation from digitized time series on a logarithmic frequency axis. *Measurement* 39(2), 120–129.
- Wiskott, L. and T. J. Sejnowski (2002). Slow Feature Analysis: Unsupervised Learning of Invariances. *Neural computation* 14(4), 715–770.